CellPress

Chemistry & Biology
Article

Maresin-like Lipid Mediators Are Produced by Leukocytes and Platelets and Rescue Reparative Function of Diabetes-Impaired Macrophages

Song Hong,[1,*] Yan Lu,[1] Haibin Tian,[1] Bhagwat V. Alapure,[1] Quansheng Wang,[1] Bruce A. Bunnell,[2] and James Monroe Laborde[3]

[1]Neuroscience Center of Excellence and Department of Ophthalmology, Louisiana State University Health Sciences Center, New Orleans, LA 70112, USA

[2]Center for Stem Cell Research and Regenerative Medicine, Tulane University School of Medicine, New Orleans, LA 70112, USA

[3]Department of Orthopedic Surgery, Louisiana State University Health Sciences Center, New Orleans, LA 70005, USA

*Correspondence: shong@lsuhsc.edu

http://dx.doi.org/10.1016/j.chembiol.2014.06.010

SUMMARY

Nonhealing diabetic wounds are associated with impaired macrophage (Mf) function. Leukocytes and platelets (PLT) play crucial roles in wound healing by poorly understood mechanisms. Here we report the identification and characterization of the maresin-like(L) mediators 14,22-dihydroxy-docosa-4*Z*,7*Z*,10*Z*,12*E*,16*Z*,19*Z*-hexaenoic acids, 14*S*,22-diHDHA (maresin-L1), and 14*R*,22-diHDHA (maresin-L2) that are produced by leukocytes and PLT and involved in wound healing. We show that 12-lipoxygenase-initiated 14*S*-hydroxylation or cytochrome P450 catalyzed 14*R*-hydroxylation and P450-initiated ω(22)-hydroxylation are required for maresin-L biosynthesis. Maresin-L treatment restores reparative functions of diabetic Mfs, suggesting that maresin-Ls act as autocrine/paracrine factors responsible for, at least in part, the reparative functions of leukocytes and PLT in wounds. Additionally, maresin-L ameliorates Mf inflammatory activation and has the potential to suppress the chronic inflammation in diabetic wounds caused by activation of Mfs. These findings provide initial insights into maresin-L biosynthesis and mechanism of action and potentially offer a therapeutic option for better treatment of diabetic wounds.

INTRODUCTION

Successful wound healing entails complex cellular and molecular processes involving diverse interactions of growth factors, cytokines, lipid mediators, resident cells, leukocytes, platelets (PLTs), and stem cells (Brem and Tomic-Canic, 2007). Soon after wounding, PLTs aggregate at the injury site to stop bleeding. Neutrophils are recruited, followed by monocytes (MCs) and other leukocytes, which prevent wound infection and/or phagocytose cell debris and infecting microbes. After infiltrating the wounds, leukocytes and PLTs can produce growth factors, cytokines, and lipid mediators that regulate fibroblasts, epithelial cells, and other resident cells as well as recruit stem cells for the repair (Hong et al., 2003; Lu et al., 2010; Phinney and Prockop, 2007). Macrophages (Mfs) in wounds are mainly differentiated from recruited blood MCs and play indispensable roles in wound healing during postnatal life. Mfs accelerate re-epithelialization by activating epithelial cells and increase granulation tissue formation by recruiting fibroblasts and endothelial cells into wounded skin (Eming et al., 2007; Koh and DiPietro, 2011).

Diabetes results in delayed healing or nonhealing of wounds. Diabetic wounds that do not heal can result in suffering, poor quality of life, and high mortality (Brem and Tomic-Canic, 2007). Diabetes impairs the molecular and cellular processes of healing, including the reparative functions of Mfs (Khanna et al., 2010; Tian et al., 2011b). Diabetic Mfs are deficient in the production of pro-healing growth factors and the promotion of wound re-epithelization and vascularization. Restoration of the reparative functions of Mfs represents a potentially effective strategy for the treatment of diabetic wounds and is a major focus of this study.

PLTs, Mfs, MCs, and polymorphonuclear neutrophils (PMNs) transform docosahexaenoic acid (DHA) into proresolution lipid mediators, which include resolvins (Serhan et al., 2002) and neuroprotectin D1/protectin D1(Hong et al., 2003; Marcheselli et al., 2003), along with 14-hydroxy-carrying maresins (Serhan et al., 2009) as well as 14-hydroxy- and ω-1-hydroxy-carrying 14,21-dihydroxy-DHAs (14,21-diHDHAs) (Lu et al., 2010). P450 ω-hydroxylases deactivate LTB_4 to 20-hydroxyl LTB_4 P450 (Capdevila et al., 2005) and convert resolvin E1 to 20-hydroxy resolvin E1 that retains bioactivity (Hong et al., 2008). Studies show that maresin1 (Serhan et al., 2009), neuroprotectin D1/protectin D1, resolvin D1 (Gronert et al., 2005; Hellmann et al., 2012; Tang et al., 2013), and 14,21-diHDHAs (Hocking, 2012; Lu et al., 2010; Tian et al., 2011a, 2011b) promote wound healing. Moreover, 14*S*,21*R*-diHDHA recovers the reparative functions of diabetic Mfs (Tian et al., 2011b). Therefore, lipid mediators may be responsible, in part, for the roles of leukocytes and PLTs in wound healing.

This background information led us to form two hypotheses addressed in this report. (1) Leukocytes and PLTs, by 12-lipoxygenase(LO)-hydroxylase and P450 ϖ-hydroxylase catalysis in tandem, convert DHA to docosanoids that carry both 14-hydroxy and ϖ-hydroxy. (2) These compounds act in an autocrine/paracrine manner that restores diabetes-impaired Mf functions in promoting the migration of epithelial cells and fibroblasts, the cellular processes known to be critical to wound healing, and in recruiting MSCs.

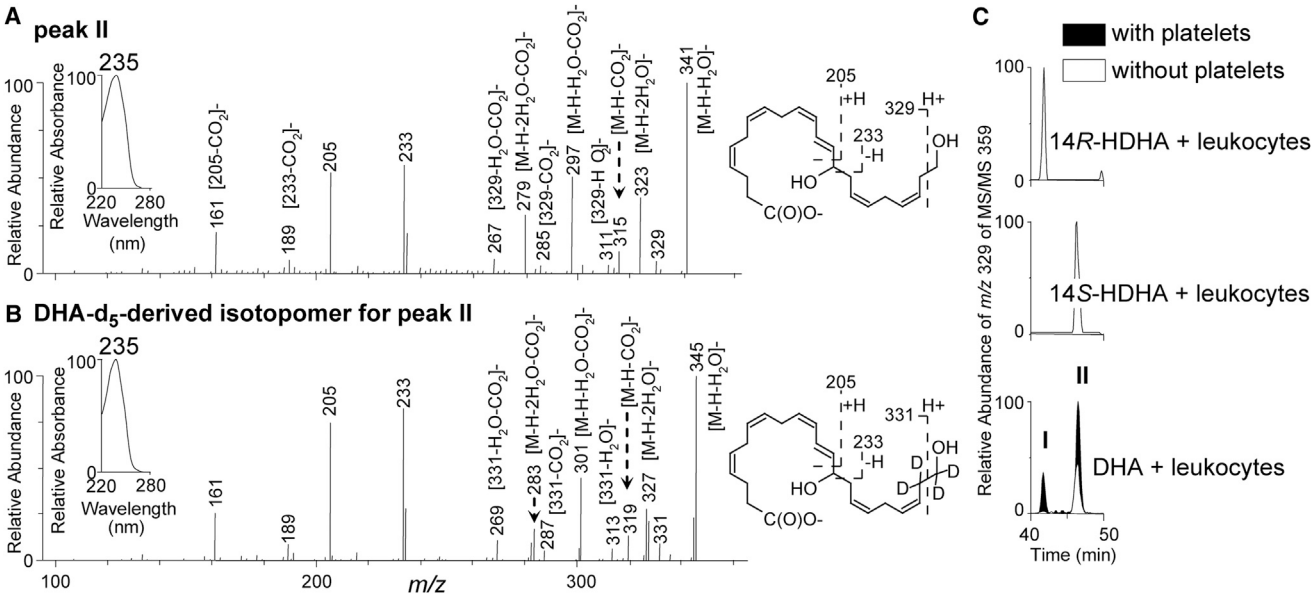

Figure 1. Structure Identification and Elucidation of 14,22-Dihydroxy-4,7,10,12,16,19-Docosahexaenoic Acids Produced from DHA by Human Leukocytes with or without Platelets

Human blood leukocytes (3×10^6 monocytes + 3×10^7 neutrophils + 3×10^6 lymphocytes) were incubated with or without 3×10^7 platelets in 3 μM DHA or DHA-*21,21,22,22,22*-d_5 and then stimulated by wound healing-relevant conditions. Leukocytes were also incubated with 3 μM 14*S*-HDHA or 14*R*-HDHA and then stimulated. The incubations were analyzed by aR chiral LC-UV-MS (AD-RH column). MS/MS and UV (inset) spectra of aR chiral LC-MS/MS chromatographic peaks demonstrate the structures (right). Diagnostic MS/MS ions are interpreted in the insets. Representative results are shown (n = 3).

(A) MS/MS UV spectra of 14,22-diHDHA for peak II in (C).

(B) MS/MS UV spectra of DHA-d_5-derived 14,22-diHDHA-d_4 corresponding to peak II in (C).

(C) Chromatograms of aR chiral LC-MS/MS for 14*R*,22-diHDHA and 14*S*,22-diHDHA generated from 14*R*-HDHA (top) and 14*S*-HDHA (center), respectively, by leukocytes or for both 14,22-diHDHAs generated from DHA (bottom) by leukocytes with or without platelets.

Fibroblasts and epithelial cells were studied here because re-epithelialization by epithelial cells is essential to covering wounds. Also, collagen deposition by fibroblasts is critical to wound healing that has high breaking strength and no dehiscence (Li et al., 2013; Ranzer et al., 2011; Yeh et al., 2009). To test these hypotheses, we studied MCs, PMNs, and lymphocytes (LYMs) isolated from human blood, Mfs from L12-LO-deficient (*L12-LO*$^{-/-}$ or *12/15-LO*$^{-/-}$) mice and wild-type controls, and type II diabetic *db/db* mice and nondiabetic *db/+* controls. We used aqueous reverse-phase chiral liquid chromatography with diode array UV spectrometry and tandem mass spectrometry (aR chiral LC-UV-MS/MS) and deuterium-labeled compounds for structure elucidation and identification of compounds. The bioactions of these compounds on *db/db* Mfs were studied regarding the promotion of migration of scratch-wounded epithelial cells and fibroblasts and transmigration of MSCs, regarding generation of hepatocyte growth factor (HGF), and regarding inflammatory activation.

RESULTS

Structure Elucidation and Identification of 14-Hydroxy and ϖ-Hydroxy-Containing Compounds Produced from n3-Docosahexaenoic Acid by Human Blood Leukocytes and Platelets

Leukocytes and PLTs play crucial reparative roles in wound healing and produce prohealing resolvins, maresins (Serhan et al., 2009), and/or 14,21-diHDHAs (Hellmann et al., 2012; Lu et al., 2010; Tian et al., 2011b). To test a part of our first hypothesis, we incubated human blood leukocytes (MCs + PMNs + LYMs) with or without PLTs in 3 μM DHA (a level found in wounds) (Tian et al., 2011a) and then activated the cells with factors involved in wound healing. The incubations were studied via aR chiral LC-UV-MS/MS. 14,22-dihydroxy 4,7,10,12,16,19-docosahexaenoic acids (14,22-diHDHAs) and their deuterium-labeled isotopomers were generated by these cells from DHA and deuterium-labeled DHA-*21,21,22,22,22*-d_5 (DHA-d_5), respectively (Figure 1). The molecular structure elucidation and identification were conducted as follows.

In the MS/MS spectra at a mass-to-charge ratio (*m/z*) 359 $[M\text{-}H]^-$ of 14,22-diHDHAs, represented by the spectrum in Figure 1A for chromatographic peak II in Figure 1C, the fragment ions *m/z* 341 $[M\text{-}H\text{-}H_2O]^-$, 323 $[M\text{-}H\text{-}2H_2O]^-$, 297 $[M\text{-}H\text{-}H_2O\text{-}CO_2]^-$, and 279 $[M\text{-}H\text{-}2H_2O\text{-}CO_2]^-$ were consistent with one carboxy and a molecular weight (M) of 360 daltons (Da). The fragment ions *m/z* 205, 161 $[205\text{-}CO_2]^-$, 233, and 189 $[233\text{-}CO_2]^-$ showed a hydroxy at the 14 position (C_{14}). Ion *m/z* 329, generated from cleavage of the C_{21}-C_{22} bond, in conjunction with ions *m/z* 311 $[329\text{-}H_2O]^-$, 285 $[329\text{-}CO_2]^-$, and 267 $[329\text{-}H_2O\text{-}CO_2]^-$, demonstrated another hydroxy at C_{22}. The identification of 14,22-diHDHA was confirmed by LC-MS/MS spectral ions of 14,22-diHDHAs-d_4 (Figure 1B), which was generated from DHA-d_5 and is illustrated in the insets for MS/MS fragmentation interpretation (Figures 1A and 1B, right insets). Fragment ions from MS/MS at *m/z* 363 $[M\text{-}H]^-$ of 14,22-diHDHAs-d_4 are *m/z* 345

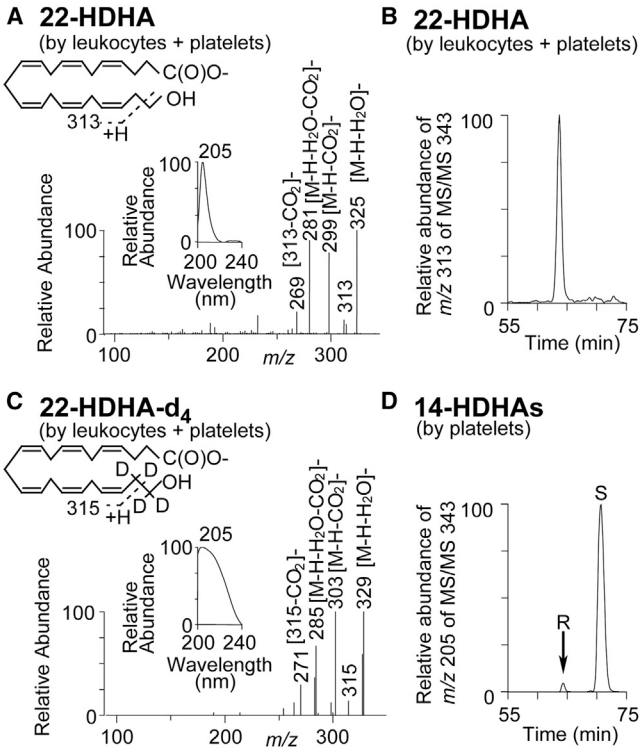

Figure 2. The Intermediates 22-HDHA, 14*R*-HDHA, and 14*S*-HDHA Were Generated from DHA by Human Blood Leukocytes plus Platelets or Platelets

Human blood platelets (3×10^7) or leukocytes + platelets (3×10^6 monocytes + 3×10^6 neutrophils + 3×10^6 lymphocytes + 3×10^7 platelets) were incubated with 3 μM DHA or DHA-*21,21,22,22,22*-d_5 and then stimulated as in Figure 1. The incubations were analyzed by aR chiral LC-UV-MS (IA column) (n = 3).

(A) 22-HDHA was identified from leukocytes + platelets by its MS/MS spectrum of the aR chiral LC-MS/MS chromatographic peak in (B).

(B) 22-HDHA produced by leukocytes + platelets, shown by its aR chiral LC-MS/MS chromatogram.

(C) MS/MS spectrum of 22-HDHA-d_4 generated from DHA-*21,21,22,22,22*-d_5.

(D) 14*S*-HDHA and 14*R*-HDHA produced by platelets shown by an aR chiral LC-MS/MS chromatogram.

$[M-H-H_2O]^-$, 327 $[M-H-2H_2O]^-$, 301 $[M-H-H_2O-CO_2]^-$, 283 $[M-H-2H_2O-CO_2]^-$, 331, 313 $[331-H_2O]^-$, 287 $[331-CO_2]^-$, 269 $[331-H_2O-CO_2]^-$, 233, 189 $[233-CO_2]^-$, 205, and 161 $[205-CO_2]^-$. One deuterium at C_{22} was replaced by 22-hydroxy, whereas the other four deuterium atoms remained at C_{21} and C_{22}, rendering the molecular ion of 14,22-diHDHA-d_4 as *m/z* 363 $[M-H]^-$. The UV spectra of 14,22-diHDHAs were consistent with that of 14,22-diHDHA-d_4, for which the maximum absorbance wavelength (λ_{max}) was 235 nm (Figures 1A and 1B, left insets), therefore confirming a pair of conjugated double bonds in their structures. Peak I in the LC-MS/MS chromatogram possessed a shorter retention time than peak II but had MS/MS and UV spectra indistinguishable from peak II. Therefore, peak I and peak II were stereoisomers of 14,22-HDHAs (Figure 1C, bottom). They were produced by human leukocytes and PLTs from DHA.

Our next aim was to determine the stereochemistry of peak I and II 14,22-HDHAs (Figure 1C, bottom). The only asymmetric carbon in the 14,22-diHDHA stereoisomers is C_{14}, which can lead to two enantiomers (14*R*,22-diHDHA and 14*S*,22-diHDHA) where the double-bond geometry of 14*S*-HDHA or 14*R*-HDHA is considered to be biosynthetically conserved, similar to the ω oxidation of eicosanoids catalyzed by P450 (Capdevila et al., 2005). A single 14,22-diHDHA aR chiral LC-MS/MS peak (Figure 1C, top) was detected, at a shorter retention time, from the incubation of 14*R*-HDHA with leukocytes. This peak possessed MS/MS and UV spectra indistinguishable from those in Figure 1A for 14,22-diHDHA. Therefore, this peak was identified as 14*R*,22-diHDHA. In parallel, a single 14,22-diHDHA aR chiral-MS/MS peak (Figure 1C, center) was also found, at a longer retention time, from incubation of 14*S*-HDHA with leukocytes. Again, this peak had MS/MS and UV spectra indistinguishable from those in Figure 1A for 14,22-diHDHA, thus, this peak was identified as 14*S*,22-diHDHA. The shorter retention time for 14*R*,22-diHDHA derived from 14*R*-HDHA (Figure 1C, top), compared with 14*S*,22-diHDHA derived from 14*S*-HDHA (Figure 1C, center), is consistent with the reports that an *R*-hydroxy enantiomer has a shorter retention time than its *S*-epimer under identical aR chiral LC conditions (Lu et al., 2010). Therefore, leukocytes with and without PLTs converted DHA to 14*R*,22-diHDHA and 14*S*,22-diHDHA.

P450 and 12-LO Are Key Enzymes in the Biosynthetic Pathways for 14*S*,22-diHDHA and 14*R*,22-diHDHA

We then tested the part of our first hypothesis that leukocytes and PLTs convert DHA to 14,22-diHDHAs by 12-LO- and P450-ω-hydroxylase catalysis in tandem or P450 alone. Based on previous information gained from the biosynthesis of 14*S*,21*R*/*S*-diHDHAs and 14*R*,21*R*/*S*-diHDHAs (Lu et al., 2010), we made three predictions. (1) The 22-hydroxy in both 14*R*,22-diHDHA and 14*S*,22-diHDHA results from P450 ω-hydroxylase, analogous to the generation of the 22-hydroxy in 22-HDHA (VanRollins et al., 1984). (2) The 14*R*-hydroxy in 14*R*,22-diHDHA is generated by P450, analogous to the 14*R*-hydroxy in P450-generated 14*R*-HDHA (Figure S1 available online). (3) 14*S*-hydroxy in 14*S*,22-diHDHA results from 12-LO-catalyzed lipoxygenation, analogous to the generation of the 14*S*-hydroxy in 14*S*-HDHA (Lu et al., 2010). Our aR chiral LC-UV-MS/MS analysis showed that human blood leukocytes and PLTs converted DHA to 22-HDHA (Figures 2A and 2B) and to 14*S*-HDHA and 14*R*-HDHA (Figure 2D) in addition to 14*S*,22-diHDHA and 14*R*,22-diHDHA (Figure 1), which is consistent with the three predictions.

22-HDHA was identified based on MS/MS ions *m/z* 269, 281, 299, 313, and 325 (Figure 2A) of the chiral LC peak detected from the incubation of leukocytes, PLTs, and DHA (Figure 2B). This observed 22-HDHA was confirmed by the 22-HDHA-d_4 biosynthesized from DHA-d_5, where 22-HDHA-d_4 possessed an LC chromatogram and MS/MS spectrum with ions *m/z* 271, 285, 303, 315, and 329 (Figure 2C), consistent with those of 22-HDHA. The UV spectrum of 22-HDHA or 22-HDHA-d_4 had a single band with λ_{max} 205 nm, consistent with the six no-conjugate double bonds in each compound (Figures 2A and 2C, insets). 22-HDHA is a marker for P450 ω-hydroxylation of DHA or DHA derivatives in leukocytes and PLTs because rat liver microsomal P450 was found to produce 22-HDHA (VanRollins et al., 1984), and auto-oxidation or oxidation catalyzed by LOs and cyclooxygenases has been found to not oxidize ω-terminal SP^3 carbon (Capdevila et al., 2005; Hong et al., 2003; Lu et al., 2010).

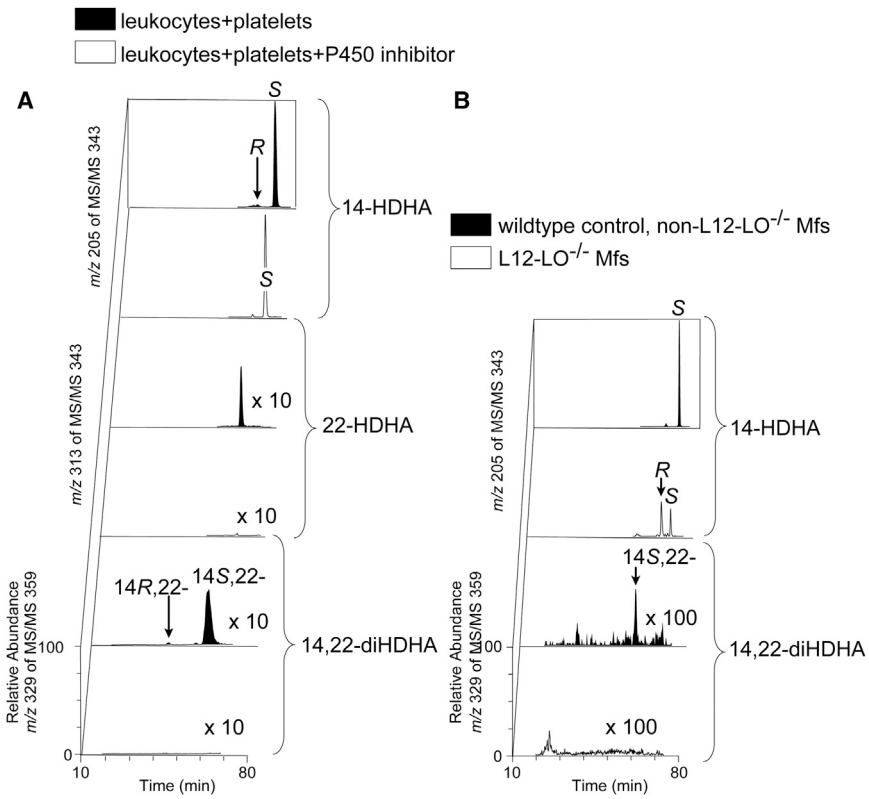

Figure 3. Identification of Pathways in the Biosynthesis of 14*S*,22-diHDHA and 14*R*,22-diHDHA

Inhibition of cytochrome P450 in leukocytes and platelets diminished production of 14*S*,22-diHDHA 14*R*,22-diHDHA, and 22-HDHA; knockout of L12-LO diminished 14*S*,22-diHDHA production by macrophages.

Human blood cells (3×10^6 monocytes + 3×10^6 neutrophils + 3×10^6 lymphocytes + 3×10^8 platelets) were incubated in 3 μM DHA and then stimulated as in Figure 1, except that the P450 inhibitor 17-ODYA or vehicle alone was added, 10 min before DHA was supplied, and added again at the same amount when stimulating. Mfs (3×10^6) isolated from *L12-LO*$^{-/-}$ or wild-type control mice were incubated in 3 μM DHA and stimulated. Incubations were analyzed via aR chiral LC-UV-MS with an IA column. Representative results are shown (n = 3).

(A) Inhibition of P450 diminished the formation of 14*S*,22-diHDHA, 14*R*,22-diHDHA, and the intermediate or biosynthetic markers 14*R*-HDHA and 22-HDHA but not 14*S*-HDHA.

(B) Knockout of L12-LO diminished Mf formation of 14*S*,22-diHDHA and its biosynthetic intermediate and marker 14*S*-HDHA.

See also Figures S1 and S2 and Table S1.

To further test our predictions, we treated the leukocytes and PLTs with the P450 inhibitor 17-octadecynoic acid (17-ODYA). This experiment confirmed the first prediction that P450 determines ω (or 22)-hydroxylation forming 14*S*,22-diHDHA, 14*R*,22-diHDHA, and 22-HDHA because P450 inhibition diminished their formation but not the formation of 14*S*-HDHA (Figure 3A). P450 inhibition also diminished the formation of 14*R*-HDHA, confirming our second prediction that P450 determines 14*R*-hydroxylation for the formation of 14*R*-HDHA and 14*R*,22-diHDHA. These results also suggest that auto-oxidation is negligible to produce 14*R*-HDHA or 14*R*,22-diHDHA under these conditions.

The quantity of 14*R*-HDHA or 14*R*,22-diHDHA generated by P450 and auto-oxidation (Figures 3A and 4) should be comparable with the amount of 14*S*-HDHA or 14*S*,22-diHDHA generated by P450 and auto-oxidation, respectively, because P450 or auto-oxidation is known to generate *S*- and *R*-enantiomers in a racemic 1:1 ratio (Kim et al., 1990). The results showed that much less 14*R*-HDHA and 14*R*,22-diHDHA than 14*S*-HDHA and 14*S*,22-diHDHA were produced by PLTs (Figures 2D and 4) and leukocytes plus PLTs (Figure 3A), respectively. Therefore, the 14*S*-HDHA or 14*S*,22-diHDHA generated by P450 and auto-oxidation should be much less than the 14*S*-HDHA or 14*S*,22-diHDHA generated by 12-LO, respectively. As such, P450 and auto-oxidation have a minor role in DHA 14*S*-hydroxylation for the biosynthesis of 14*S*,22-diHDHA. Leukocytes and PLT converted 14*S*-HDHA to 14*S*,22-HDHA (Figure 1C, center). Therefore, our data support the third prediction for the dominant role of 12-LO in forming 14*S*-hydroxy of 14*S*,22-diHDHA.

To further test this, we incubated DHA with peritoneal Mfs isolated from *L12-LO*$^{-/-}$ and wild-type control mice and analyzed extracts with aR chiral LC-UV-MS/MS. The *L12-LO*$^{-/-}$ Mfs were deficient in the production of 14*S*,22-diHDHA and its biosynthetic intermediate or pathway marker 14*S*-HDHA, whereas wild-type Mfs produced 14*S*,22-diHDHA and 14*S*-HDHA (Figure 3B). Because auto-oxidation, P450, cyclooxygenases, and 5-LO are not abolished by the *L12-LO*$^{-/-}$, the diminished formation of 14*S,22*-diHDHA and 14*S*-HDHA in Mfs by *L12-LO*$^{-/-}$ suggests that auto-oxidation, P450, cyclooxygenases, and 5-LO are insignificant or ineffective in DHA 14*S*-hydroxylation for biosynthesis of 14*S*,22-diHDHA and 14*S*-HDHA. Together, these data substantially confirm our third prediction that 12-LO is a key enzyme required for 14*S*-hydroxylation in the biosynthesis of 14*S*,22-diHDHA. Our immunohistological analysis of wounded mouse or human skin showed that Mfs and PMNs expressed L12-LO or the human equivalent, h15-LO-1 (Funk et al., 2002), respectively (Figure S2 and Table S1), demonstrating the existence of L12-LO- or h15-LO-1-expressing Mfs and PMNs in wounds for potential biosynthesis of 14*S*,22-diHDHA.

We sought to identify the specific P450 responsible for the biosynthesis of 14,22-diHDHAs by incubating DHA or 14*S*/*R*-HDHA with a human cytochrome P450 enzyme (h-P450) mixture (BioCatalytics). The h-P450 mixture contained NADPH cofactor and six h-P450s in fixed ratios (recombinant human CYP1A2, 2C8, 2C9, 2D6, 2E1, and 3A4). Targeted lipidomic analysis with aR chiral LC-UV-MS/MS of the incubations showed that these P450s did not generate 14,22-diHDHAs and nor did the biosynthesis of the intermediate 22-HDHA, However, they converted DHA to the intermediates 14*S*-HDHA and 14*R*-HDHA in

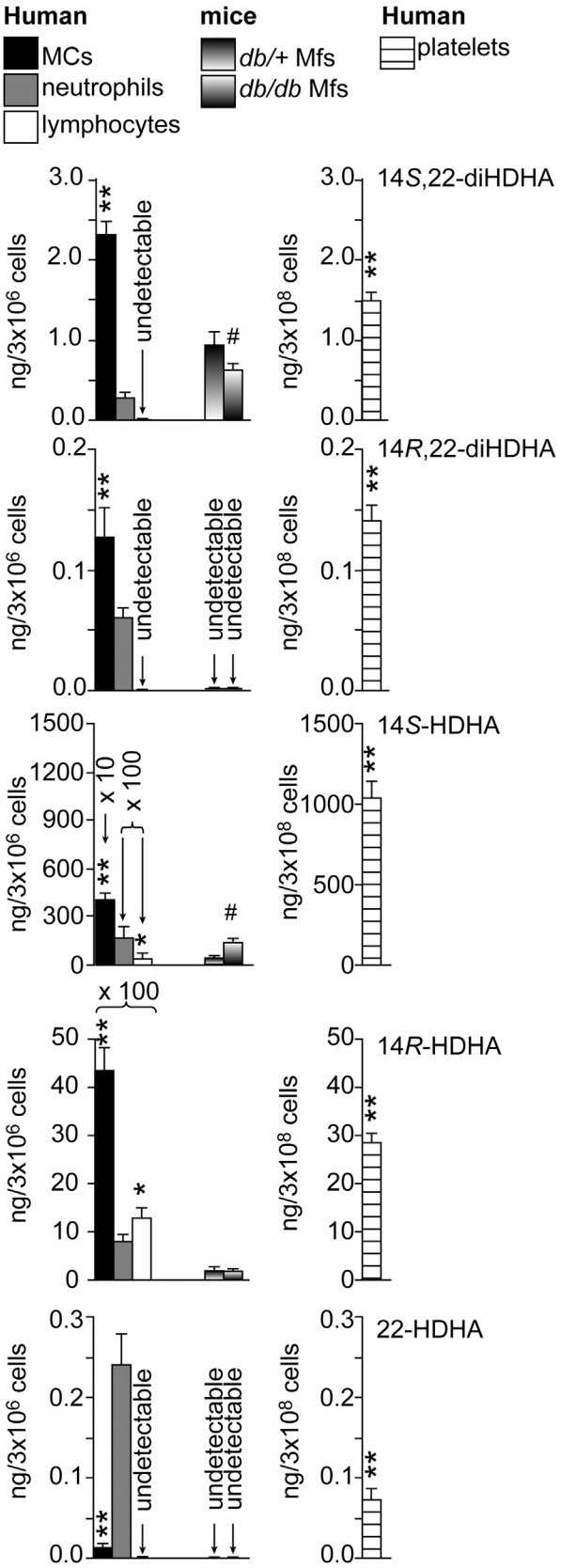

Figure 4. Differential Activities of Human Monocytes, Neutrophils, Lymphocytes, or Platelets or Macrophages of Diabetic *db/db* or Nondiabetic *db/+* Mice in Producing 14*S*,22-diHDA, 14*R*,22-diHDHA, and the Biosynthetic Intermediates or Markers 22-HDHA, 14*S*-HDHA, and 14*R*-HDHA

Human MCs (3×10^6), neutrophils (3×10^6), lymphocytes (3×10^6), or platelets (3×10^8) or Mfs of *db/db* or *db/+* mice were incubated in 3 μM DHA and then stimulated as in Figure 1. The incubations were analyzed using aR chiral LC-UV-MS. For Mfs of *db/db* or *db/+* mice, the medium also contained 25 mM glucose. Results are mean ± SEM (n = 4). *p < 0.05, **p < 0.01 versus neutrophils; #p < 0.05 versus *db/+* Mfs.
See also Figures S2 and S3 and Table S1.

a racemic 1:1 ratio (Figure S1). Therefore, human CYP1A2, 2C8, 2C9, 2D6, 2E1, and 3A4 did not catalyze 22-hydroxylation/ω-oxidation of either DHA, 14*S*-HDHA, or 14*R*-HDHA but did catalyze 14*S*-hydroxylation and 14*R*-hydroxylation of DHA, which could contribute to the biosynthesis of 14,22-diHDHAs from DHA. However, as we concluded above, the amount of 14*S*-hydroxylation catalyzed by P450 is relatively minor compared with the amount catalyzed by P12-LO in PLTs and L12-LO or h15-LO-1 in leukocytes.

Different Activities of Monocytes, PMNs, Lymphocytes, and Platelets of Humans as well as Macrophages of Diabetic and Nondiabetic Mice in the Biosynthesis of 14*S*,22-DiHDA and 14*R*,22-DiHDHA

To compare the activities of human PLTs, PMNs, LYMs, and MCs (Mf precursors) in the biosynthesis of 14*S*,22-diHDA and 14*R*,22-diHDHA from DHA, we quantified them and their biosynthetic intermediates or markers 14*S*-HDHA, 14*R*-HDHA, and 22-HDHA following incubation with DHA (wound level) (Figure 4). MCs produced ~8 times as much 14*S*,22-diHDHA and twice as much 14*R*,22-diHDHA compared with PMNs, whereas LYMs did not produce a detectable amount of 14,22-diHDHAs. The blood of healthy humans contains ~3×10^8 PLTs/ml and ~6×10^6 leukocytes/ml (Handin et al., 2003). We found that 3×10^8 PLTs produced ~65% as much 14*S*,22-diHDHA as 3×10^6 MCs but a similar amount of 14*R*,22-diHDHA. Biosynthesis of the 14S-HDHA intermediate by PLTs and MCs was at much higher levels than by PMNs or LYMs, which correlated with the production of 14*S*,22-diHDHA by these populations. Biosynthesis of 14*R*-HDHA (14*R*,22-diHDHA intermediate) by PLTs and MCs exhibited a trend similar to that of 14*S*-HDHA levels. Biosynthesis of 22-HDHA (an intermediate of both 14*S*,22-diHDHA and 14*R*,22-diHDHA) was highest in PMNs, lower in PLTs, much lower in MCs, and undetectable in LYMs. Levels of 14*S*,22-diHDHA produced by MCs, PMNs, or PLTs were ~17, ~4, or ~9 times higher than the respective levels of 14*R*,22-diHDHA. Therefore, the rank order with respect to biosynthesis of 14*S*,22-diHDHA and 14*R*,22-HDHA was MCs (3×10^6 cells) ≥ PLT (3×10^8 cells) > PMN (3×10^6 cells). The data also suggest that LYMs do not produce these molecules at a detectable level. Human plasma alone did not contain or produce detectable 14*S*/*R*,22-diHDHA but can modestly promote 14*S*/*R*,22-diHDHA production by blood cells, although it did not change above the rank order (Figure S3).

Mfs differentiate from MCs and are able to convert DHA to 14,22-diHDHAs (Figure 3B). In an autocrine/paracrine manner, Mfs produce lipid mediators and then use the lipid mediators

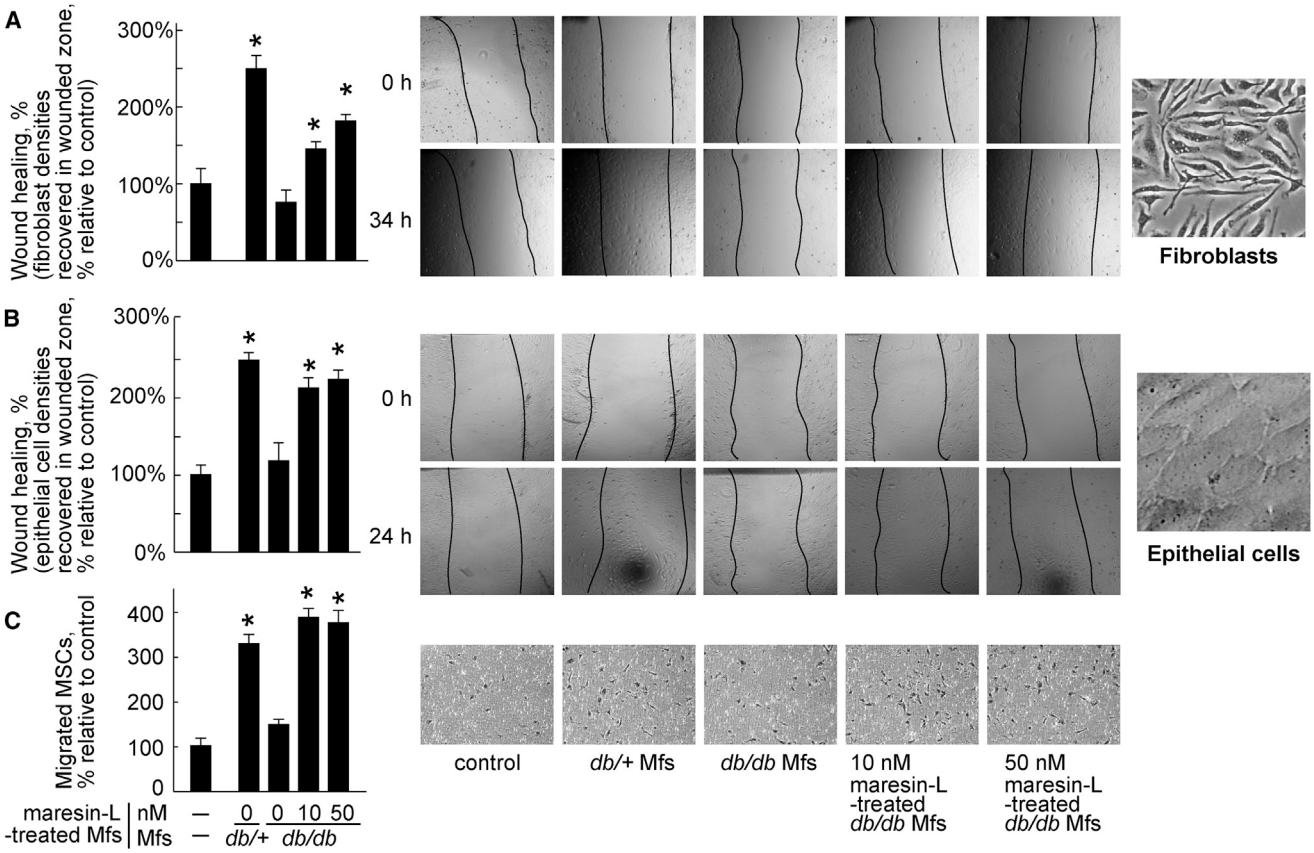

Figure 5. Maresin-L, 14,22-diHDHA, Treatment Restored Diabetes-Impaired *db/db* Macrophage Functions in Promoting Wound Healing and in Recruiting MSCs

Mfs were isolated from diabetic *db/db* or nondiabetic control *db/+* mice. Scratch wounds were generated in the monolayers of fibroblasts and epithelial cells in dishes, which were then treated for 34 and 24 hr, respectively, with CM from *db/db* or *db/+* Mfs cultured without or with maresin-Ls (14,22-diHDHAs) (0, 10, or 50 nM). Wound healing was percent of cell densities recovered in the original wound zone relative to the control without CM. MSC transmigration was started by adding murine MSCs into the upper chambers of transwells and adding CM of *db/db* or *db/+* Mfs cultured without or with 14,22-diHDHAs (0, 10, or 50 nM) into the lower chamber. The transmigration was expressed as percent of migrated MSCs relative to control without CM. Results are mean ± SEM (n = 4). *p < 0.01 compared with CM of *db/db* Mfs without maresin-L treatment. Quantitative results are shown on the left, and representative microphotographs are shown in the center. The cell morphologies are shown on the right.

(A) Scratch wound healing of fibroblasts in CM of Mfs.

(B) Scratch wound healing of epithelial cells in CM of Mfs.

(C) Transmigration of MSCs toward CM of Mfs.

to regulate their self-functions as well as functions of other cells (Serhan et al., 2009; Tian et al., 2011b). We predicted that diabetes may affect Mf production of 14,22-diHDHAs because diabetes impairs Mf functions. This prediction was tested by comparative studies of Mfs of diabetic *db/db* mice and nondiabetic control *db/+* mice. We found that *db/+* Mfs produced more 14*S*,22-diHDHA from DHA than *db/db* Mfs (Figure 4), indicating that there was a deficiency of 14,22-diHDHA generation by diabetic Mfs. 25 mM glucose for 24 hr did not affect *db/+* Mf production of 14,22-diHDHA compared with 5 mM glucose (data not shown).

Bioactions of 14,22-diHDHAs on Diabetes Impaired Reparative Functions of Macrophages

Because Mfs, MCs, PMNs, and PLTs produce 14,22-diHDHAs and play crucial roles in healing (Figures 1, 3, and 4), because diabetes impairs Mf 14,22-diHDHA-formation (Figure 4) and reparative functions, and because Mf-produced 14*S*,21*R*-diHDHA restores the functions of diabetic Mfs (Tian et al., 2011b), we were motivated to test our second hypothesis that 14,22-diHDHAs act as autocrine/paracrine factors capable of restoring diabetes-impaired Mf functions. We assessed the effect of 14,22-diHDHAs on the reparative functions of Mfs from diabetic *db/db* mice in wound healing of fibroblasts or epithelial cells. Mfs from diabetic *db/db* mice were treated with 14,22-diHDHAs (14*S*,22-diHDHA:14*R*,22-diHDHA, 10:1) at different concentrations (24 hr, 37°C). The medium from the Mf cultures was used as Mf-conditioned medium (CM). 14,22-diHDHAs were undetectable by aR chiral LC-MS/MS in the medium after conditioning. Compared with the conditioned medium from nondiabetic *db/+* Mfs, the conditioned medium from diabetic *db/db* Mfs was incapable of promoting the migration of scratch-wounded fibroblasts (Figure 5A) or epithelial cells (Figure 5B). However, treatment of *db/db* Mfs with 14,22-diHDHAs,

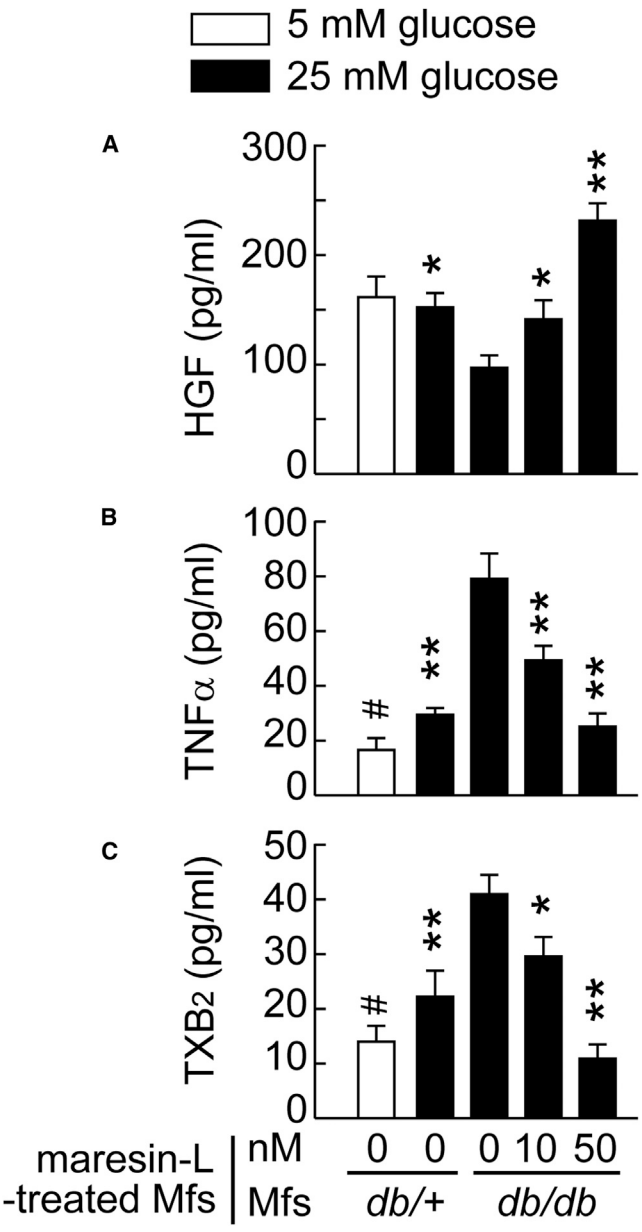

Figure 6. Maresin-L, 14,22-diHDHA, Treatment Increased *db/db* Macrophage Expression of HGF but Decreased *db/db* Macrophage Production of TNFα and TXB_2 under Hypoxia and High-Glucose Conditions Relevant to Diabetic Wounds

Macrophages (Mfs) isolated from diabetic *db/db* or nondiabetic control *db/+* mice were cultured in medium containing 0, 10, or 50 nM maresin-Ls and 25 mM glucose under hypoxia (95% N_2, 5%CO_2, 24 h). For comparison, Mfs isolated from nondiabetic *db/+* mice were cultured in medium without maresin-Ls and with normal glucose (5 mM) under hypoxia (95% N_2, 5%CO_2, 24 h). The Mf-conditioned media were analyzed for HGF, TNFα, and TXB_2 by ELISA. Results are mean ± SEM (n = 3). *p < 0.05, **p < 0.01 compared with CM of *db/db* Mfs without maresin-L treatment; #p < 0.05 compared with CM of *db/+* Mfs without maresin-L treatment and with normal glucose.

(A) HGF.

(B) TNFα.

(C) TXB_2.

even at concentrations as low as 10 nM, restored the reparative activity of *db/db* Mfs on promoting migration of scratch-wounded fibroblasts or epithelial cells. Both 14,22-diHDHAs and maresins are 14-hydroxy-carrying autocrine/paracrine docosanoids of Mfs because they are produced by Mfs and regulate Mfs (Serhan et al., 2009). Maresins also potently enhance Mf reparative functions. Therefore, 14,22-diHDHAs are denoted "maresin-like (maresin-L)."

We next studied the effect of maresin-Ls on *db/db* Mf migration of MSCs using a transmigration assay because MSCs can accelerate healing by producing paracrine factors and replenishing cells lost in wounds (Phinney and Prockop, 2007). Conditioned medium from nondiabetic *db/+* Mfs stimulated transmigration of MSCs from the upper chamber, whereas conditioned medium from diabetic *db/db* Mfs did not. However, conditioned medium from *db/db* Mfs treated with maresin-Ls, in a nanomolar range, enabled *db/db* Mfs to produce conditioned medium that significantly stimulated transmigration of MSCs from the upper chamber (Figure 5C). Therefore, maresin-L treatment could rescue diabetes-impaired functions of Mfs in recruiting MSCs.

Activated Mfs produce HGF (Yin et al., 2014), which accelerates wound healing and MSC migration. We postulated that a plausible mechanism by which maresin-Ls restored the reparative functions of *db/db* Mfs might, in part, be augmenting prohealing growth factor production. To test this, we used ELISA to quantify HGF in conditioned medium from *db/db* and *db/+* Mfs and maresin-L-treated *db/db* Mfs. The results showed that HGF secretion by *db/db* Mfs was significantly less than by *db/+* Mfs under simulated selected diabetic wound conditions (hypoxia and high glucose) (Figure 6A), consistent with the impaired functions of *db/db* Mfs (Figure 5). The deficiency of *db/db* Mfs was corrected by treatment with maresin-Ls, which promoted HGF production in a dose-dependent manner (Figure 6A). This recovery of HGF production may be involved in the rescue of *db/db* Mf functions in wound healing and MSC transmigration (Figure 5).

Excessive chronic inflammation and sustained inflammatory activation of Mfs are major causes of nonhealing of diabetic wounds (Khanna et al., 2010; Tian et al., 2011b). Diabetic *db/db* Mfs produced significantly more inflammatory tumor necrosis factor α (TNFα) and thromboxane A_2 (TXA_2, detected as its stable derivative, TXB_2) compared with nondiabetic *db/+* Mfs under simulated selected diabetic wound conditions (Figures 6B and 6C), indicating excessive inflammatory activation of *db/db* Mfs. At the nanomolar range, maresin-Ls considerably reduced the levels of TNFα and TXA_2 produced by *db/db* Mfs in a dose-dependent manner (Figures 6B and 6C). These data indicate that maresin-Ls reduced inflammatory activation of diabetic Mfs by reducing their TNFα and TXA_2 production, which could be beneficial in the healing of diabetic wounds. Culture with 25 mM glucose for 24 hr increased *db/+* Mf production of TNFα and TXB_2 but had no effect on HGF production.

DISCUSSION

The Maresin-like Docosanoids 14*S*,22-diHDHA and 14*R*,22-diHDHA Are Generated by Leukocytes and Platelets

The cellular and molecular mechanisms for the crucial roles of leukocytes and PLTs in injury repair are emerging and remain

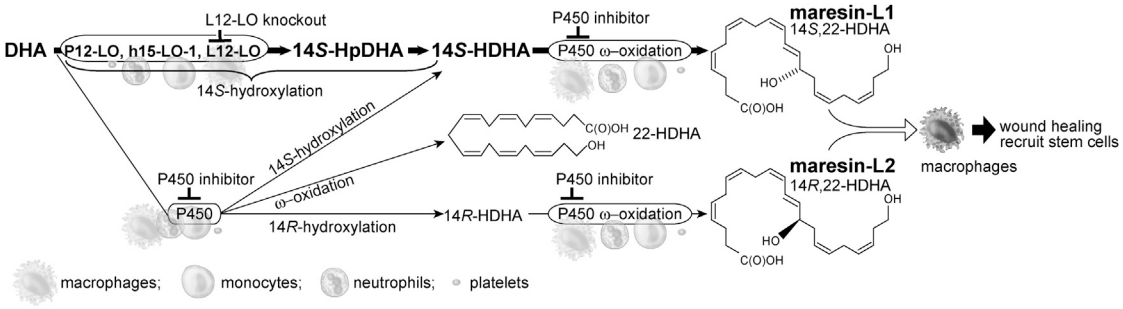

Figure 7. Schematic Outlining the Tentative Biosynthetic Pathways and Bioactions of ω-Hydroxy Maresin-like Docosahexaenoic Mediators Generated by Leukocytes and Platelets

DHA is transformed by leukocytes and platelets via h15-LO-1 or L12-LO (12/15-LO) and P12-LO, respectively, to 14*S*-hydroperoxy-DHA (14*S*-HpDHA), which is reduced to 14*S*-HDHA. These cells further convert 14*S*-HDHA to 14*S*,22-diHDHA (maresin-L1) through P450-catalyzed ω(22)-oxidation. Alternatively, by P450 activities of the cells, DHA is first transformed to 14*S*-HDHA, 14*R*-HDHA, and 22-HDHA. Then 14*R*-HDHA is converted by P450 to 14*R*,22-diHDHA (maresin-L2). The double bond geometries of 14*S* (or *R*)-HDHA are conserved after being converted to maresin-Ls based on our results and reported analogous data for eicosanoids. This conservation also applies to the transformation of DHA to 22-HDHA. Maresin-Ls represent autocrine/paracrine factors that are produced by monocytes, macrophages, neutrophils, and/or platelets. They act on macrophages in the promotion of wound healing and MSC transmigration. See also Figure S4.

to be elucidated further. In this study, we identified and characterized two ω-hydroxy docosahexaenoids, 14*S*,22-diHDHA (maresin-L1) and 14*R*,22-diHDHA (maresin-L2), that are generated from DHA by leukocytes and/or PLTs. We performed structural elucidation by aR chiral LC-UV-MS/MS spectroscopy and chromatography, including use of deuterium-labeled isotopomers (Wang et al., 2013). The chiralities of the two 14,22-diHDHA stereoisomers were identified. The knowledge of activities of PLTs and each type of leukocyte in 14,22-diHDHA biosynthesis are the basis to harnessing these activities for wound healing treatment.

Our data indicate different capabilities for biosynthesis of 14*S*,22-diHDHA and 14*R*,22-HDHA by different cell types. We found that the rank of production was MCs ≥ PLTs > PMNs. LYMs did not produce these molecules at a detectable level. These findings suggest differential contributions from different blood cells for generation of 14,22-diHDHAs and differential roles for 14,22-diHDHAs as autocrine or paracrine factors in the functions of these cells in wound healing.

P450 and 12-LO Are Responsible for the Biosynthesis of Maresin-L1 and Maresin-L2 by Leukocytes and Platelets

Based on the results, we propose tentative biosynthetic pathways for 14,22-diHDAs (Figure 7; Figure S4). We found that inhibition of P450 of leukocytes and PLTs and knockout of L12-LO in murine Mfs suggest the following. (1) P450 is responsible for 22-hydroxylation/ω-oxidation to produce 14,22-diHDHAs from either DHA, 14*S*-HDHA, or 14*R*-HDHA as well as for 14*R*-hydroxylation to produce 14*R*,22-diHDHA from DHA or 22-HDHA. (2) Auto-oxidation, cyclooxygenases, and 5-LO are negligible for the biosynthesis of these compounds. P450 plays a minor role in DHA 14*S*-hydroxylation for biosynthesis of 14*S*,22-diHDHA and 14*S*-HDHA. This is consistent with a previous report showing that cyclooxygenases did not produce 14-HDHA (Serhan et al., 2002). (3) P12-LO, L12-LO, and/or h15-LO-1 have a dominant role, whereas P450 has a minor role in DHA 14*S*-hydroxylation for the biosynthesis of 14*S*,22-diHDHA. These results are consistent with a report showing that LO inhibition by esculetin or *L12-LO*$^{-/-}$ blocks formation of 14*S*-HDHA from DHA in leukocyte-rich exudates from peritonitis (Serhan et al., 2009).

Out data indicate that human CYP1A2, 2C8, 2C9, 2D6, 2E1, and 3A4 do not catalyze 22-hydroxylation of DHA or 14*R*/*S*-HDHA but catalyze DHA 14*R*/*S*-hydroxylation (Figure S1), although the 14*S*-hydroxylation catalyzed by P450 is much less than that catalyzed by P12-LO in PLTs and h15-LO-1 or L12-LO in leukocytes. It is very likely that the 22-hydroxylation of DHA or 14*S*/*R*-HDHA for 14,22-diHDHA biosynthesis are catalyzed by the P450 CYP4 family because these P450s are responsible for ω-hydroxylation of fatty acids and eicosanoids (Kikuta et al., 2002). Moreover, CYP4F is expressed in human leukocytes (Kikuta et al., 2004). Mouse CYP4F18 is an ortholog of human PMN CYP4F3A (Christmas et al., 2006). CYP1A1, 2U1, 2J2, 4A11, 4F2, and 5A1 are expressed as both proteins and mRNAs in PLTs (Jarrar et al., 2013). Systematic studies are needed to define the specific P450s responsible for 14,22-diHDHA formation in leukocytes and PLTs.

The major enzymes for the biosynthesis of DHA-derived mediators in human MCs and PMNs are 5-LO, h15-LO-1, and P450, whereas, in mouse Mfs, they are 5-LO, L12-LO, and P450. In PLTs, they are P12-LO and P450 (Ikei et al., 2012; Serhan et al., 2009). Our data suggest that the h15-LO-1 in human leukocytes, L12-LO in mouse Mfs, and P12-LO in PLTs were responsible for DHA 14*S*-hydroxylation for 14*S*,22-diHDHA biosynthesis. The ratio of 14*S*-HDHA to 14*S*,22-diHDHA, as produced by PLTs, is 1017/1.5 ≈670, whereas, for MCs or PMNs, it is 40/2.3 ≈17 or 1.7/0.3 ≈6, respectively (Figure 4). Consequently, the excess PLT-produced 14*S*-HDHA may be transferred to adjacent leukocytes and converted by leukocytes to 14*S*,22-HDHA, similar to the transcellular biosynthesis of lipoxins by PLTs and leukocytes (Serhan and Romano, 1995).

A number of Mfs and PMNs expressed L12-LO or h15-LO-1, respectively, in wounded skin of mice or humans (Figures S2A–S2D). We also found intermediates or pathway markers, 14*R*/*S*-HDHA and 22-HDHA, for the biosynthesis of 14,22-diHDHAs in mouse wounded skin (Figures S2E and S2F).

However, 14,22-diHDHAs were undetectable. It is likely that 14,22-diHDHAs might be produced by the Mfs and PMNs in wounds via L12-LO or h15-LO-1. If so, then these molecules might have acted on local cells and been degraded by the tissue before our analysis.

In aggregate (Figure 7), our results indicate that the biosynthesis of 14*S*,22-diHDHA by PLTs and leukocytes includes 14*S*-hydroxylation of DHA, which is determined by P12-LO and L12-LO or h15-LO-1, respectively. The 14*S*-HDHA is then hydroxylated at C_{22} by MCs, PLTs, and/or PMNs via P450 to 14*S*,22-diHDHA. Alternatively, by P450, DHA is first converted to 14*S*-HDHA, 14*R*-HDHA, and 22-HDHA, and then, the last two are further converted to 14*R*,22-diHDHA. 22-HDHA could be converted to 14*S*,22-diHDHA via 14*S*-hydroxylation as above. It could also be converted to 14*R*,22-diHDHA via 14*R*-hydroxylation catalyzed by P450 (Figure S3). The double bond geometries of DHA, 14*R*/*S*-HDHAs, and 22-HDHA are conserved after conversion of the intermediates to 14,22-diHDHAs, based on our results and according to reported analogous data for eicosanoids (Capdevila et al., 2005; Hong et al., 2003). Therefore, 14,22-diHDHAs produced by leukocytes and/or PLTs are 14*S*/*R*,22-dihydroxy docosa-4*Z*,7*Z*,10*Z*,12*E*,16*Z*,19*Z*-hexaenoic acids.

Maresin-L1 and Maresin-L2 Act as Autocrine/Paracrine Factors to Diminish Diabetic Impairment of Macrophage Reparative Functions

We sought to identify natural lipid molecules produced by leukocytes and PLTs that can diminish the diabetic impairment of Mf reparative functions. Diabetic *db*/*db* Mfs were deficient in promoting migration of epithelial cells and fibroblasts and in the transmigration of MSCs compared with nondiabetic *db*/+ Mfs (Figure 5), which was associated with the deficiency of 14,22-diHDHA (maresin-L) production by *db*/*db* Mfs (Figure 4). Treating *db*/*db* Mfs with maresin-Ls recovered the Mf reparative capabilities. These results suggest that maresin-Ls, as autocrine/paracrine factors produced by PLTs and leukocytes, including Mfs, act on Mfs to diminish the diabetic impairment of Mf reparative functions. Furthermore, the association of decreased formation of maresin-Ls with impaired reparative functions of *db*/*db* Mfs suggests that the impairment of Mf function in diabetes also involves an impaired formation of these autocrine/paracrines. 14*S*/*R*,22-diHDHA is likely to mainly affect wound healing locally after the blood cells enter the wounds because 14*S*/*R*,22-diHDHA is likely to be produced by these cells, mostly in wounds where there were more stimuli than in the circulation as injury stimuli come from wounds. However, if the wounding is severe enough to change the blood microenvironment, as severe burns do, it may activate blood cells to produce sufficient amounts of 14*S*/*R*,22-diHDHA in the circulation, which may have systemic effects on healing.

Maresin-L treatment ameliorates the diabetic impairment of Mf production of HGF, a growth factor that regulate the cellular processes responsible for wound repair, including stem cell transmigration, re-epithelialization, angiogenesis, and collagen deposition. The mechanism by which maresin-Ls restore Mf reparative functions in diabetes may include the promotion of Mf HGF expression. This implies that maresin-Ls restore diabetes-impaired paracrine functions in *db*/*db* Mfs.

Diabetic wounds are characterized by chronic inflammation and sustained inflammatory activation of Mfs (Brem and Tomic-Canic, 2007), exemplified by increased production of inflammatory TNFα and TXA_2 by *db*/*db* Mfs (Figures 6B and 6C). Chronic inflammation in wounds retards the healing process and damages tissue and is largely responsible for delayed healing of diabetic wounds. Maresin-Ls reduced TNFα and TXA_2 generation by diabetic Mfs. Our results suggest that maresin-Ls produced by leukocytes and PLTs are likely able to reduce the excess inflammatory activation of diabetic Mfs, which is the major driver of chronic inflammation in the middle and late healing phases in diabetic wounds (Khanna et al., 2010). Therefore, maresin-Ls could also promote healing by reducing chronic inflammation via an Mf-associated mechanism.

The ratio of M2 to M1-like Mfs is higher in *db*/+ wounds than that in *db*/*db* wounds (Bannon et al., 2013), and M2 Mfs express much more 12/15-LO than M1 Mfs (Biswas and Mantovani, 2012). Therefore, the diabetes-reduced population percentage of M2-like or 12/15-LO-expressing Mfs may contribute to the deficiency of 14,22-diHDHA production by *db*/*db* Mfs. However, diabetes may also dysregulate the P450s for the biosynthesis and metabolism of 14,22-diHDHA, similar to the dysregulation of enzyme systems involved in the biosynthesis and metabolism of eicosanoids (Kämpfer et al., 2005; Kapoor et al., 2006). These potential mechanisms need to be studied systematically studied in the future.

In this report, we studied the actions of maresin-Ls in vitro. We focused on the actions of factors secreted from Mfs after treatment with maresin-Ls. However, the direct contact of Mfs with other cells may have additional consequences and should be studied systematically. Maresin-Ls may also be active on other leukocytes, such as T cells, PMNs, master cells, dendritic cells, and so forth, which also deserve to be investigated. The thioglycollate-elicited peritoneal Mfs used here exhibit some similarities to skin wound Mfs on the studied aspects, including the diabetes-affected production of TNFα and IL10 as well as the promotion of diabetic wound healing (Khanna et al., 2010; Koh and DiPietro, 2011; Tian et al., 2011b). This is consistent with diabetes-impaired phagocytosis by zymosan-elicited Mfs of *db*/*db* mice (Tang et al., 2013). However, rat wound Mfs can induce apoptosis of PMNs. Rat *Propionibacterium acnes*-elicited peritoneal Mfs cannot induce PMN apoptosis (Meszaros et al., 1999), indicating that there is a possible behavior difference between mouse wound macrophages and mouse thioglycollate-elicited peritoneal Mfs in regard to PMN apoptosis. Therefore, our results using thioglycollate-elicited peritoneal Mfs should be confirmed further by in vivo experiments of skin wound healing in conjunction with using skin wound Mfs. Nonetheless, our results are of translational significance because they appear to provide a basis for further preclinical studies on the application of maresin-Ls for restoration of diabetes-impaired Mf reparative functions in diabetic wounds. The regulatory mechanisms governing the bioactions of each maresin-L on diabetic Mf functions related to the impairment of injury repair need to be elucidated.

Our findings may provide mechanistic insights for reparative functions of leukocytes and PLTs and provide molecular structure templates of maresin-Ls (14,22-diHDHAs) that may prove valuable in the development of therapeutics for the treatment of diabetic wounds (Brem and Tomic-Canic, 2007; Martin, 1997).

SIGNIFICANCE

Leukocytes and PLTs play crucial roles in wound healing by mechanisms that need to be determined further. We identified two maresin-L docosahexaenoic mediators, 14*S*,22-diHDHA (maresin-L1) and 14*R*,22-diHDHA (maresin-L2), and demonstrated their potential to restore diabetes-impaired Mf reparative functions. Maresin-Ls are biosynthesized by MCs, Mfs, PLTs, and PMNs. We found that the biosynthetic pathways for maresin-Ls require 12-LO-initiated 14*S*-hydroxylation or cytochrome P450-catalyzed 14*R*-hydroxylation and P450-catalyzed ω(22)-hydroxylation of DHA. Maresin-L treatment restores reparative functions to diabetic Mfs, enabling their promotion of migration of fibroblasts and epithelial cells, the cellular processes known to be critical to wound healing, and migration of mesenchymal stem cells via mechanisms that may include enhancement of Mf production of HGF. Maresin-L treatment also ameliorates the inflammatory activation of diabetic Mfs. Therefore, maresin-Ls have the potential to suppress the chronic inflammation in diabetic wounds caused by inflammatory activation of Mfs. These data suggest that maresin-Ls act as autocrine/paracrine factors responsible for, at least in part, the reparative functions of leukocytes and PLTs in wounds. These findings may provide mechanistic insights into the roles of leukocytes and PLTs in wound healing and offer a therapeutic option of using maresin-L-rescued diabetic Mfs for better treatment of diabetic wounds.

EXPERIMENTAL PROCEDURES

Materials

DHA, DHA-d_5, 14*R/S*-HDHA, and 17-ODYA were from Cayman.

Animals

All procedures involving animals followed animal protocols approved by the Institutional Animal Care and Use Committees of our institutes. Diabetic *db/db* (BKS.Cg-m+/+leprdb) and nondiabetic *db*/+ mice (11 weeks old, female) (Jackson Laboratory) were used when blood glucose was 25–35 mM for *db/db* mice and 5–10 mM for *db*/+ mice. *L12-LO*$^{-/-}$ and wild-type C57BL/6J control mice were 11-week-old females (Jackson Laboratory).

Isolation of Human Platelets, PMNs, Monocytes, and Lymphocytes

Human samples were obtained following protocols approved by the Institutional Review Boards of our institutes. Established procedures were followed (Hong et al., 2003; Serhan and Romano, 1995). Human whole blood provided by the Blood Center was from a healthy donor who was unknown to us and who had not been on medication for >2 weeks prior to donation. The blood in sodium citrate was centrifuged (180 × *g*, 10 min, 23°C). Then the supernatants were centrifuged (1100 × *g*, 15 min, 23°C). The top layer was plasma. Cell pellets were washed with 7 mM EDTA, which yielded PLTs with a purity of 1 leukocyte/3 × 10^4 PLTs. PMNs and mononuclear cells were isolated from blood by Ficoll-Hypague gradient. The mononuclear cells were plated onto plastic dishes. The cells adhered to the dishes were MCs. and nonadhered cells were LYMs. The PMNs, MCs, and LYMs prepared were of >96% purity. The viability of cells was >95% according to trypan blue exclusion.

Isolation of Mouse Macrophages

Mouse Mfs were isolated and identified as reported previously (Tian et al., 2011b). Mice (*db/db*, *db*/+, *L12-LO*$^{-/-}$, or C57BL/6J) were treated with thioglycollate for 3 days. Cells were collected by peritoneal lavage and plated in RPMI 1640 medium onto plastic dishes (24 hr, 37°C, 5% CO_2). The adherent cells were harvested, which yielded more than 95% F4/80$^+$ Mfs (Tian et al., 2011b).

Biosynthesis of Docosanoids

14*S*-HDHA was generated from DHA by porcine L12-LO (Cayman) and isolated by aR chiral LC-UV-MS/MS (Thermo Scientific) with an AD-RH or IA chiral column (150 mm long × 2.1 mm inner diameter × 5 μm, Chiral Tech) (Lu et al., 2010), or 14*S*-HDHA and 14*R*-HDHA were separated from racemic 14*S/R*-HDHAs (Cayman) by aR chiral-LC-UV-MS/MS (Lu et al., 2010). In experiments involving cellular production of docosanoids, human PMNs (3 × 10^6), MCs (3 × 10^6), LYMs (3 × 10^6), PLTs (3 × 10^8), leukocytes (3 × 10^6 PMNs + 3 × 10^6 MCs + 3 × 10^6 LYMs), leukocytes plus PLTs (3 × 10^6 PMNs + 3 × 10^6 MCs + 3 × 10^6 LYMs + 3 × 10^8 PLTs), or Mfs (3 × 10^6) of *L12-LO*$^{-/-}$, C57BL6, *db/db,* or *db*/+ mice were incubated (20 min, 37°C) in PBS containing 3 μM DHA, DHA-d_5, 14*S*-HDHA, or 14*R*-HDHA. The cells were then stimulated (37°C, 30 min) with 10 ng/ml TNFα, 10 ng/ml IL-1β, 100 ng/ml lipopolysaccharide, and 1 U/ml thrombin (if PLTs were added). For Mfs of *db/db* or *db*/+ mice, the media contained 25 mM glucose to simulate diabetic hyperglycemia or 5 mM for normal glucose control. DHA has been reported to be ~3 μmol/kg in wounded skin of *db*/+ and *db/db* mice (Tian et al., 2011a). Therefore, 3 μM DHA is physiologically relevant to wound healing. To inhibit P450, human leukocytes plus PLTs (3 × 10^6 PMNs + 3 × 10^6 MCs + 3 × 10^6 LYMs + 3 × 10^8 PLTs) were treated with a P450 inhibitor, 50 μM 17-ODYA, or vehicle control (0.005% DMSO) (10 min, 37°C) (Chiang et al., 1998; Muerhoff et al., 1989). The incubation was continued for 20 min after adding DHA (3 μM), followed by addition of the same amount of 17-ODYA. Then it was stimulated as above.

Analysis and Preparation of 14,22-diHDHAs Using aR Chiral LC-UV-MS/MS

The final incubations were extracted and analyzed or fractionated for docosanoids using aR chiral LC-UV-MS/MS, as we published previously (Lu et al., 2010; Tian et al., 2011a). For the AD-RH column, the mobile phase flowed at 0.15 ml/min. It eluted as D (acetonitrile:H_2O:acetic acid = 45:55:0.01) from 0–45 min, ramped to acetonitrile from 45.1–60 min, and then flowed as acetonitrile. For the IA column, the mobile phase flowed at 0.2 ml/min, eluted as B (methanol:H2O:acetic acid = 27:73:0.01) from 0–1 min, ramped from B:methanol 40:60 to B:methanol 20:80 by 50 min, ramped to methanol by 55 min, and then flowed as methanol. The incubation of leukocytes plus PLTs with DHA were fractionated using the same aR chiral LC-UV-MS/MS as for the preparation of 14,22-diHDHAs. The isolated 14*S*,22-diHDHA or 14*R*,22-diHDHA were 98% pure based on LC-UV-MS/MS analysis. 14*S*,22-diHDHA and 14*R*,22-diHDHA purified from incubations of [leukocytes + PLTs + DHA] were of an ~10:1 ratio (in nanomoles) and, therefore, combined in a 10:1 ratio for the studies of their bioactions. Prostaglandin E_2-d_4 (5 ng) was added to each incubation as an internal standard for quantification after the biosynthesis was stopped by methanol.

Conditioned Medium of Macrophages Treated by Hypoxia and 14,22-diHDHAs and Analysis of HGF, TNFα, and TXB_2

db/db and *db*/+ Mfs (3 × 10^5) were incubated in a hypoxia chamber (95% N_2, 5%CO_2) in fresh RPMI 1640 with 25 or 5 mM glucose and 14,22-diHDHAs at 0, 10, or 50 nM (24 hr). The final medium after the removal of debris did not contain detectable 14,22-diHDHAs and was used as the conditioned medium. HGF, TNFα, and TXB_2 in conditioned medium were analyzed by ELISA kits (R&D Systems). The hypoxia simulated the low O_2 levels found in wounded tissue (Fife et al., 2009; Kang et al., 2013).

Scratch Wounding In Vitro

Established procedures were followed with minor adjustments (Kenchegowda et al., 2011). Mouse fibroblasts (CF-1, ATCC) and human epithelial cells (HK2, ATCC) were grown to confluence in Eagle's minimal essential medium with 15% fetal bovine serum (FBS) and DMEM/Ham's F12 with 10% FBS, respectively. Then each cell line was starved to quiescence in 0.5% FBS (12 hr, 37°C). Quiescent cell monolayers were scratch-wounded using a sterile 200 μl pipette tip to generate a cell-denuded wound zone, washed, and incubated with medium containing 0.5% FBS and 20% conditioned medium of Mfs treated without or with 14,22-diHDHAs (0, 10, or 50 nM). The wound was allowed to heal for 34 hr (for fibroblasts) or 24 hr (for epithelial cells), a point at which cells inside the wound zone for different conditions had reached 0%–90% confluence. The wounded areas were photographed under a phase contrast microscope at ×20 magnification. The wound healing was quantified

as the percentage of cell densities recovered in the original cell-denuded wound zone relative to a control without conditioned medium (Tomic-Canic et al., 2007).

Isolation of MSCs from Mice and Transmigration of MSCs

MSCs were isolated as described in our prior publications, and more than 95% of isolated MSCs were positive for Sca-1 and CD29 based on flow cytometric analysis (Izadpanah et al., 2006; Tian et al., 2011a, 2012). Previously published procedures were followed, with minor modifications, for the assay of MSC transmigration (Kim et al., 2010). Briefly, mouse MSCs (4×10^5) were added into the upper chamber of 24-well transwell plates (8 μm). Murine mesenchymal medium (STEMCELL Technologies) (600 μl), and conditioned medium (200 μl) from Mfs treated without or with 14,22-diHDHAs (0, 10, 50 nM) was added into the lower chamber. Migration was carried out for 4 hr at 37°C. The cells underneath the membrane were stained with Giemsa and counted as migrated cells. Migration was measured as cell number per five microscope fields. Results are expressed as percent migrated MSCs compared to control without conditioned medium.

Statistics

Results are reported as mean ± SEM and were analyzed by ANOVA, followed by Fisher's least significant difference post hoc comparison. $p < 0.05$ was considered significant.

SUPPLEMENTAL INFORMATION

Supplemental Information includes Supplemental Experimental Procedures, four figures, and one table and can be found with this article online at http://dx.doi.org/10.1016/j.chembiol.2014.06.010.

ACKNOWLEDGMENTS

This research was funded by NIH Grant R01-DK087800 (to S.H.) and Research to Prevent Blindness, New York. We thank Drs. Nicolas G. Bazan and Haydee E.P. Bazan for providing the *L12-LO*$^{-/-}$ mice, Mr. Ryan Labadens and Yue-Liang Brewerton for editing, and Shirley N. Hong for graphic assistance.

Received: April 6, 2014
Revised: May 25, 2014
Accepted: June 9, 2014
Published: September 4, 2014

REFERENCES

Bannon, P., Wood, S., Restivo, T., Campbell, L., Hardman, M.J., and Mace, K.A. (2013). Diabetes induces stable intrinsic changes to myeloid cells that contribute to chronic inflammation during wound healing in mice. Dis. Model. Mech. *6*, 1434–1447.

Biswas, S.K., and Mantovani, A. (2012). Orchestration of metabolism by macrophages. Cell Metab. *15*, 432–437.

Brem, H., and Tomic-Canic, M. (2007). Cellular and molecular basis of wound healing in diabetes. J. Clin. Invest. *117*, 1219–1222.

Capdevila, J.H., Holla, V.R., and Faick, J.R. (2005). Cytochrome P450 and the metabolism and bioactivation of arachidonic acid and eicosanoids. In Cytochrome P450: Structure, Mechanism, and Biochemistry, R.O.d.M. Paul, ed. (New York: Kluwer Academic/Plenum Publishers).

Chiang, N., Takano, T., Clish, C.B., Petasis, N.A., Tai, H.H., and Serhan, C.N. (1998). Aspirin-triggered 15-epi-lipoxin A4 (ATL) generation by human leukocytes and murine peritonitis exudates: development of a specific 15-epi-LXA4 ELISA. J. Pharmacol. Exp. Ther. *287*, 779–790.

Christmas, P., Tolentino, K., Primo, V., Berry, K.Z., Murphy, R.C., Chen, M., Lee, D.M., and Soberman, R.J. (2006). Cytochrome P-450 4F18 is the leukotriene B4 omega-1/omega-2 hydroxylase in mouse polymorphonuclear leukocytes: identification as the functional orthologue of human polymorphonuclear leukocyte CYP4F3A in the down-regulation of responses to LTB4. J. Biol. Chem. *281*, 7189–7196.

Eming, S.A., Krieg, T., and Davidson, J.M. (2007). Inflammation in wound repair: molecular and cellular mechanisms. J. Invest. Dermatol. *127*, 514–525.

Fife, C.E., Smart, D.R., Sheffield, P.J., Hopf, H.W., Hawkins, G., and Clarke, D. (2009). Transcutaneous oximetry in clinical practice: consensus statements from an expert panel based on evidence. Undersea Hyperb. Med. *36*, 43–53.

Funk, C.D., Chen, X.S., Johnson, E.N., and Zhao, L. (2002). Lipoxygenase genes and their targeted disruption. Prostaglandins Other Lipid Mediat. *68-69*, 303–312.

Gronert, K., Maheshwari, N., Khan, N., Hassan, I.R., Dunn, M., and Laniado Schwartzman, M. (2005). A role for the mouse 12/15-lipoxygenase pathway in promoting epithelial wound healing and host defense. J. Biol. Chem. *280*, 15267–15278.

Handin, R.I., Lux, S.E., and Stossel, T.P. (2003). Blood: Principles and Practice of Hematology, Second Edition. (Philadelphia: Lippincott Williams and Wilkins), p. 471.

Hellmann, J., Tang, Y., and Spite, M. (2012). Proresolving lipid mediators and diabetic wound healing. Curr. Opin. Endocrinol. Diabetes Obes. *19*, 104–108.

Hocking, A.M. (2012). Mesenchymal Stem Cell Therapy for Cutaneous Wounds. Adv Wound Care (New Rochelle) *1*, 166–171.

Hong, S., Gronert, K., Devchand, P.R., Moussignac, R.L., and Serhan, C.N. (2003). Novel docosatrienes and 17S-resolvins generated from docosahexaenoic acid in murine brain, human blood, and glial cells. Autacoids in anti-inflammation. J. Biol. Chem. *278*, 14677–14687.

Hong, S., Porter, T.F., Lu, Y., Oh, S.F., Pillai, P.S., and Serhan, C.N. (2008). Resolvin E1 metabolome in local inactivation during inflammation-resolution. J. Immunol. *180*, 3512–3519.

Ikei, K.N., Yeung, J., Apopa, P.L., Ceja, J., Vesci, J., Holman, T.R., and Holinstat, M. (2012). Investigations of human platelet-type 12-lipoxygenase: role of lipoxygenase products in platelet activation. J. Lipid Res. *53*, 2546–2559.

Izadpanah, R., Trygg, C., Patel, B., Kriedt, C., Dufour, J., Gimble, J.M., and Bunnell, B.A. (2006). Biologic properties of mesenchymal stem cells derived from bone marrow and adipose tissue. J. Cell. Biochem. *99*, 1285–1297.

Jarrar, Y.B., Cho, S.A., Oh, K.S., Kim, D.H., Shin, J.G., and Lee, S.J. (2013). Identification of cytochrome P450s involved in the metabolism of arachidonic acid in human platelets. Prostaglandins Leukot. Essent. Fatty Acids *89*, 227–234.

Kämpfer, H., Schmidt, R., Geisslinger, G., Pfeilschifter, J., and Frank, S. (2005). Wound inflammation in diabetic ob/ob mice: functional coupling of prostaglandin biosynthesis to cyclooxygenase-1 activity in diabetes-impaired wound healing. Diabetes *54*, 1543–1551.

Kang, S., Lee, D., Theusch, B.E., Arpey, C.J., and Brennan, T.J. (2013). Wound hypoxia in deep tissue after incision in rats. Wound Repair Regen. *21*, 730–739.

Kapoor, M., Kojima, F., Appleton, I., Kawai, S., and Crofford, L.J. (2006). Major enzymatic pathways in dermal wound healing: current understanding and future therapeutic targets. Curr. Opin. Investig. Drugs *7*, 418–422.

Kenchegowda, S., Bazan, N.G., and Bazan, H.E. (2011). EGF stimulates lipoxin A4 synthesis and modulates repair in corneal epithelial cells through ERK and p38 activation. Invest. Ophthalmol. Vis. Sci. *52*, 2240–2249.

Khanna, S., Biswas, S., Shang, Y., Collard, E., Azad, A., Kauh, C., Bhasker, V., Gordillo, G.M., Sen, C.K., and Roy, S. (2010). Macrophage dysfunction impairs resolution of inflammation in the wounds of diabetic mice. PLoS ONE *5*, e9539.

Kikuta, Y., Kusunose, E., and Kusunose, M. (2002). Prostaglandin and leukotriene omega-hydroxylases. Prostaglandins Other Lipid Mediat. *68-69*, 345–362.

Kikuta, Y., Yamashita, Y., Kashiwagi, S., Tani, K., Okada, K., and Nakata, K. (2004). Expression and induction of CYP4F subfamily in human leukocytes and HL60 cells. Biochim. Biophys. Acta *1683*, 7–15.

Kim, H.Y., Karanian, J.W., Shingu, T., and Salem, N., Jr. (1990). Stereochemical analysis of hydroxylated docosahexaenoates produced by human platelets and rat brain homogenate. Prostaglandins *40*, 473–490.

Kim, Y.S., Kwon, J.S., Hong, M.H., Kim, J., Song, C.H., Jeong, M.H., Cho, J.G., Park, J.C., Kang, J.C., and Ahn, Y. (2010). Promigratory activity of oxytocin on

umbilical cord blood-derived mesenchymal stem cells. Artif. Organs *34*, 453–461.

Koh, T.J., and DiPietro, L.A. (2011). Inflammation and wound healing: the role of the macrophage. Expert Rev. Mol. Med. *13*, e23.

Li, J., Ollague Sierra, J., Zhu, L., Tang, L., Rahill, K., El-Sabawi, B., Liu-Mares, W., Mertz, P.M., and Davis, S.C. (2013). Effects of a topical aqueous oxygen emulsion on collagen deposition and angiogenesis in a porcine deep partial-thickness wound model. Exp. Dermatol. *22*, 674–676.

Lu, Y., Tian, H., and Hong, S. (2010). Novel 14,21-dihydroxy-docosahexaenoic acids: structures, formation pathways, and enhancement of wound healing. J. Lipid Res. *51*, 923–932.

Marcheselli, V.L., Hong, S., Lukiw, W.J., Tian, X.H., Gronert, K., Musto, A., Hardy, M., Gimenez, J.M., Chiang, N., Serhan, C.N., and Bazan, N.G. (2003). Novel docosanoids inhibit brain ischemia-reperfusion-mediated leukocyte infiltration and pro-inflammatory gene expression. J. Biol. Chem. *278*, 43807–43817.

Martin, P. (1997). Wound healing–aiming for perfect skin regeneration. Science *276*, 75–81.

Meszaros, A.J., Reichner, J.S., and Albina, J.E. (1999). Macrophage phagocytosis of wound neutrophils. J. Leukoc. Biol. *65*, 35–42.

Muerhoff, A.S., Williams, D.E., Reich, N.O., CaJacob, C.A., Ortiz de Montellano, P.R., and Masters, B.S. (1989). Prostaglandin and fatty acid omega- and (omega-1)-oxidation in rabbit lung. Acetylenic fatty acid mechanism-based inactivators as specific inhibitors. J. Biol. Chem. *264*, 749–756.

Phinney, D.G., and Prockop, D.J. (2007). Concise review: mesenchymal stem/multipotent stromal cells: the state of transdifferentiation and modes of tissue repair—current views. Stem Cells *25*, 2896–2902.

Ranzer, M.J., Chen, L., and DiPietro, L.A. (2011). Fibroblast function and wound breaking strength is impaired by acute ethanol intoxication. Alcohol. Clin. Exp. Res. *35*, 83–90.

Serhan, C.N., and Romano, M. (1995). Lipoxin biosynthesis and actions: role of the human platelet LX-synthase. J. Lipid Mediat. Cell Signal. *12*, 293–306.

Serhan, C.N., Hong, S., Gronert, K., Colgan, S.P., Devchand, P.R., Mirick, G., and Moussignac, R.L. (2002). Resolvins: a family of bioactive products of omega-3 fatty acid transformation circuits initiated by aspirin treatment that counter proinflammation signals. J. Exp. Med. *196*, 1025–1037.

Serhan, C.N., Yang, R., Martinod, K., Kasuga, K., Pillai, P.S., Porter, T.F., Oh, S.F., and Spite, M. (2009). Maresins: novel macrophage mediators with potent antiinflammatory and proresolving actions. J. Exp. Med. *206*, 15–23.

Tang, Y., Zhang, M.J., Hellmann, J., Kosuri, M., Bhatnagar, A., and Spite, M. (2013). Proresolution therapy for the treatment of delayed healing of diabetic wounds. Diabetes *62*, 618–627.

Tian, H., Lu, Y., Shah, S.P., and Hong, S. (2011a). 14S,21R-dihydroxydocosahexaenoic acid remedies impaired healing and mesenchymal stem cell functions in diabetic wounds. J. Biol. Chem. *286*, 4443–4453.

Tian, H., Lu, Y., Shah, S.P., and Hong, S. (2011b). Autacoid 14S,21R-dihydroxy-docosahexaenoic acid counteracts diabetic impairment of macrophage prohealing functions. Am. J. Pathol. *179*, 1780–1791.

Tian, H., Lu, Y., Shah, S.P., Wang, Q., and Hong, S. (2012). 14S,21R-dihydroxy-docosahexaenoic acid treatment enhances mesenchymal stem cell amelioration of renal ischemia/reperfusion injury. Stem Cells Dev. *21*, 1187–1199.

Tomic-Canic, M., Mamber, S.W., Stojadinovic, O., Lee, B., Radoja, N., and McMichael, J. (2007). Streptolysin O enhances keratinocyte migration and proliferation and promotes skin organ culture wound healing in vitro. Wound Repair Regen. *15*, 71–79.

VanRollins, M., Baker, R.C., Sprecher, H.W., and Murphy, R.C. (1984). Oxidation of docosahexaenoic acid by rat liver microsomes. J. Biol. Chem. *259*, 5776–5783.

Wang, M., Han, R.H., and Han, X. (2013). Fatty acidomics: global analysis of lipid species containing a carboxyl group with a charge-remote fragmentation-assisted approach. Anal. Chem. *85*, 9312–9320.

Yeh, J., Green, L.M., Jiang, T.X., Plikus, M., Huang, E., Chang, R.N., Hughes, M.W., Chuong, C.M., and Tuan, T.L. (2009). Accelerated closure of skin wounds in mice deficient in the homeobox gene Msx2. Wound Repair Regen. *17*, 639–648.

Yin, J., Lee, J.H., Zhang, J., Gao, Z., Polotsky, V.Y., and Ye, J. (2014). Regulation of hepatocyte growth factor expression by NF-kB and PPARγ in adipose tissue. Am. J. Physiol. Endocrinol. Metab. *306*, E929–E936.